Letter

# Accurate Neural Network Description of Surface Phonons in Reactive Gas−Surface Dynamics: N$_2$ + Ru(0001)

Khosrow Shakouri,*,[†] Jörg Behler,[‡] Jörg Meyer,[†] and Geert-Jan Kroes*,[†]

[†]Gorlaeus Laboratories, Leiden Institute of Chemistry, Leiden University, P.O. Box 9502, 2300 RA Leiden, The Netherlands
[‡]Universität Göttingen, Institut für Physikalische Chemie, Theoretische Chemie, Tammannstrasse 6, 37077 Göttingen, Germany

**S** *Supporting Information*

**ABSTRACT:** Ab initio molecular dynamics (AIMD) simulations enable the accurate description of reactive molecule−surface scattering especially if energy transfer involving surface phonons is important. However, presently, the computational expense of AIMD rules out its application to systems where reaction probabilities are smaller than about 1%. Here we show that this problem can be overcome by a high-dimensional neural network fit of the molecule−surface interaction potential, which also incorporates the dependence on phonons by taking into account all degrees of freedom of the surface explicitly. As shown for N$_2$ + Ru(0001), which is a prototypical case for highly activated dissociative chemisorption, the method allows an accurate description of the coupling of molecular and surface atom motion and accurately accounts for vibrational properties of the employed slab model of Ru(0001). The neural network potential allows reaction probabilities as low as $10^{-5}$ to be computed, showing good agreement with experimental results.
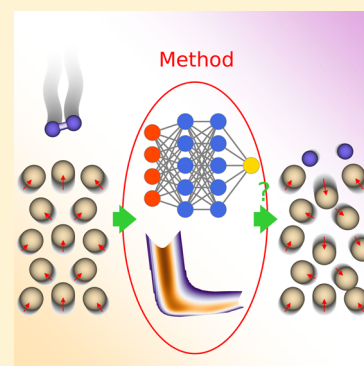
The accurate simulation of atomic and molecular scattering from metal surfaces often requires a reliable description of surface phonon motion,[1−4] especially if the projectile is heavier than dihydrogen. Although it may often be possible to obtain reasonably accurate descriptions of the scattering dynamics with a reduced dimensionality representation of the surface vibrations,[5] for quantitative agreement, it is mandatory to use an ab initio molecular dynamics (AIMD) approach.[6,7] AIMD recently enabled a chemically accurate description of the reaction of CHD$_3$ with Ni(111).[8] The high accuracy of AIMD stems from its ability to include the motion of the atoms in the upper surface layers by computing the interatomic forces on-the-fly through electronic structure methods, which for molecules scattering from metal surfaces usually rely on density functional theory (DFT).[9] However, AIMD is computationally expensive, presently making simulations of long-lasting or low-probability chemical processes infeasible. This poses a severe challenge: how can we enable AIMD-quality simulations of molecule−surface reaction processes associated with low probabilities at affordable computational costs?

Here we address this question for the N$_2$ + Ru(0001) reaction, which is considered a paradigm for highly activated dissociative adsorption. Dissociation of N$_2$ over Ru surfaces is also of practical interest as this reaction is the rate-determining step in ammonia synthesis, for which Ru is an efficient catalyst.[10,11] The N$_2$ + Ru(0001) system has therefore received a lot of attention in a series of experimental studies.[12−18] These experiments have shown that the dissociation probability $S_0$ of N$_2$ is very small (for the collisional energy range of ∼1−2.75 eV, the measured values are $S_0 \approx 10^{-6}-10^{-3}$),[16−18] even though the minimum barrier height is only about 1.8 eV.[17,19,20] It has been suggested that the low reactivity is due to

nonadiabatic effects, such as electron−hole pair excitation.[21] Subsequent quasi-classical trajectory (QCT) calculations carried out within the Born−Oppenheimer static surface (BOSS) approximation showed that the low reactivity could be well explained by the barrier representing an extremely narrow bottleneck to reaction.[19,20] However, discrepancies between theory and experiment remained, and it was suggested that surface phonons might play an important role.[19,20]

As simulating the low probability N$_2$ + Ru(0001) reaction with AIMD would require running too many (∼5 × 10$^5$) expensive AIMD trajectories, instead we investigate the role of phonons by developing a DFT-quality high-dimensional (HD) neural network potential (NNP) for N$_2$ + Ru(0001). The applicability of artificial neural networks to describing chemical reactions has already been proven for, for example, bulk materials,[22,23] organic reactions,[24,25] simulations of solid−liquid interfaces,[26] molecules interacting with static surfaces,[27−29] and, very recently, energy transfer to metal surfaces in scattering of HCl from Au(111).[30] However, in the latter molecule−surface scattering study, reaction probabilities and scattering probabilities were not yet calculated, although final rotational state distributions in scattering were presented. In this work, for the first time, we apply the HD-NNP approach to reactive molecule−surface scattering with inclusion of surface atom motion.

Here, in order to construct a HD-NNP for N$_2$ + Ru(0001), we employ the method of Behler−Parrinello,[31] through which the energy is expressed as a sum of environmentally dependent

atomic energies, and the atomic environments are described by many-body atom-centered symmetry functions.[32,33] The accuracy of the HD-NNP is assessed by comparison with the DFT reference data for $N_2$ + Ru(0001) as well as with available experimental results regarding the phonons of Ru. After this validation step, the HD-NNP is used to generate reaction probabilities for comparison with experiments[17,18] and to quantitatively analyze the role of phonons and the surface temperature ($T_s$).

The HD-NNP is developed from a data set of 25 000 $N_2$ + Ru(0001) structures, including the concomitant information on their energy and forces. To obtain the data, we carried out DFT calculations with the RPBE functional[34] as implemented in the Vienna Ab initio Simulation Package (VASP),[35−38] which was also used in earlier studies.[19,20] The DFT calculations used a 3 × 3 surface unit cell and seven atomic layers of Ru atoms, of which the bottom layer was kept stationary while the $N_2$ molecule was placed on the top side of the slab. The calculations employed a plane wave cutoff of 550 eV and a 7 × 7 × 1 Γ-point centered mesh of k-points.

The HD-NNP was constructed using the RuNNer package.[32,39] The DFT data included 5000 configurations of two nitrogen atoms on an ideally frozen surface and 20 000 configurations on the thermally disordered Ru(0001) surface. For the latter, the thermal displacements of the atoms from their equilibrium positions were sampled randomly from a Gaussian distribution, making sure to also include data for surface temperatures (up to $T_s$ = 900 K) higher than those used in the experiments simulated below (up to $T_s$ = 600 K). For both the N and the Ru atoms, radial and angular symmetry functions were used to describe interactions with neighbor atoms within their chemical environment up to a cutoff radius of 5.82 Å.[31,32]

As a first test of the HD-NNP, we examine two-dimensional (2D) cuts through the potential energy surface (PES), showing it as a function of the molecular coordinates $r$ and $Z$ (see Figure 1a) for impact on the bridge site at two different orientations of the molecule (Figure 1b,c). The 2D cuts provided by the HD-NNP are compared with DFT data computed on a fine grid and then interpolated with splines. In this particular case, the surface atoms were kept frozen at their equilibrium positions to facilitate the comparison. The dissociation geometries studied are close to the minimum barrier geometry found in ref 40. Direct comparison shows that the HD-NNP accurately predicts the DFT data for the geometries and the static surface configuration considered. To check whether a similar accuracy is obtained also for other dissociation geometries and for distorted surface geometries, the 25 000 points on which the HD-NNP is based was divided in a test set of 5000 points (which were picked at random from the complete set) and a training set of 20 000 points. With the fit based on the training set, the total energy of each structure present in the test data set was evaluated and a root-mean-square (RMS) deviation of 38 meV (less than 1 kcal/mol) from the DFT data was obtained for the total energies. The same or higher accuracy is expected from the HD-NNP constructed with the aid of the complete set, which was used in the reactive scattering calculations reported below.

The so-constructed HD-NNP also accurately describes vibrational properties of the Ru(0001) slab, as evidenced by the corresponding phonon band structure and density of states. Our phonon calculations are based on the so-called "direct method"[42] as implemented in an in-house version of the
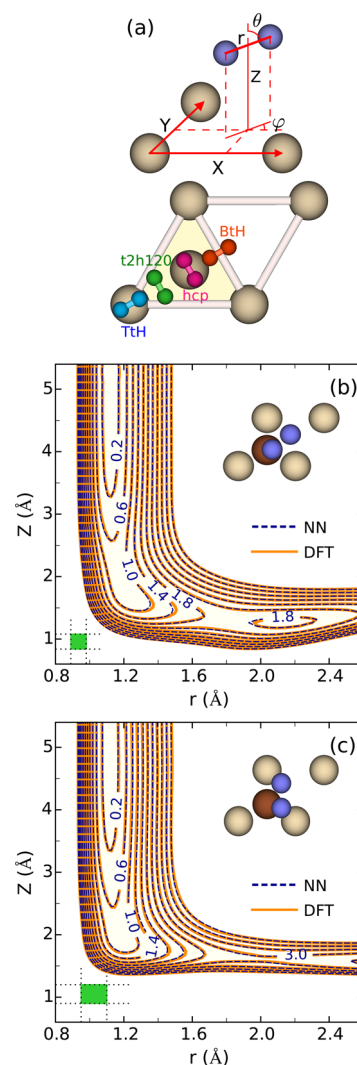


**Figure 1.** (a) Illustration of molecular coordinates in the center of mass system and of four dissociation geometries. (b,c) 2D elbow maps of the PES, for $N_2$ on Ru(0001), as a function of the ($r$, $Z$) coordinates for $\theta$ = 80° and $\varphi$ = 40° (b) and for $\theta$ = $\varphi$ = 90° (c). The blue dashed and orange solid curves describe the HD-NNP and the spline interpolated raw DFT data, respectively. The mesh size used for the interpolation is specified as a green rectangle. The insets schematically depict the orientation of $N_2$ with respect to the surface. The energy difference between successive contour lines is 0.4 eV.

phonopy code,[43,44] interfacing both the VASP and LAMMPS[45] codes and using the same computational setups as described before. We have verified that 3 × 3 multiples of the surface unit cell yield converged phonon band structures and densities of states. The results for the phonon band structure are summarized in Figure 2a for the path given by the high-symmetry points $\overline{\Gamma}-\overline{K}-\overline{M}-\overline{\Gamma}$ through the surface Brillouin zone and compared with the results obtained directly from RPBE-DFT calculations and with experimental results (ref 41). Note that for accurate extraction of the phonon dispersion relation, the RMS error in the interatomic forces, from which the required force constants are derived, should be less than 0.001 eV/Å. The acoustic phonon mode frequencies in Figure 2a obtained from the HD-NNP are in excellent agreement with both the RPBE-DFT and the experimental results.[41] Likewise, the frequencies of the highest optical phonon modes at point $\overline{\Gamma}$, that is, $\omega(\overline{\Gamma}) \approx 31-32$ meV, are consistent with the results
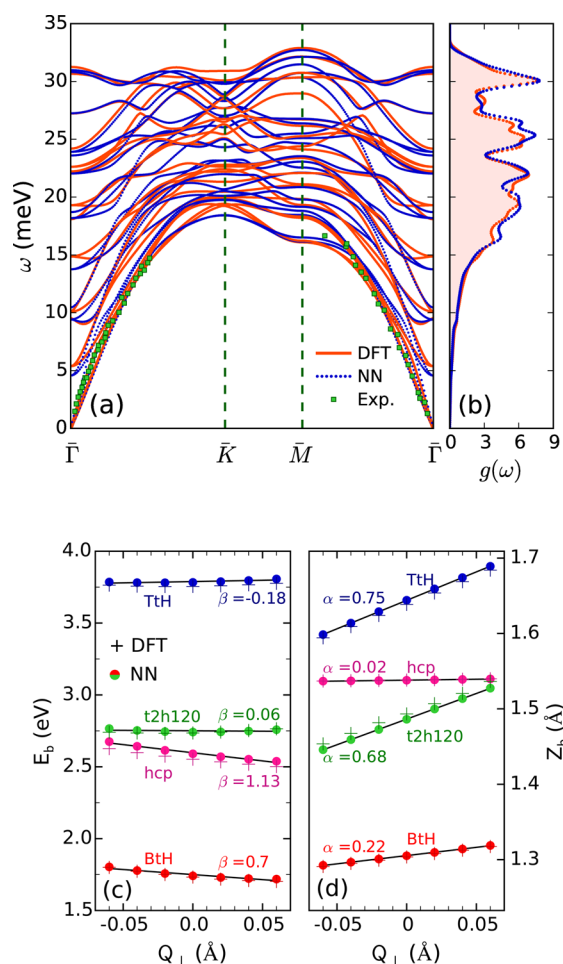
**Figure 2.** (a) Phonon dispersion of Ru(0001) along the path through the surface Brillouin zone given by the high-symmetry points $\bar{\Gamma}-\bar{K}-\bar{M}-\bar{\Gamma}$. The blue dots are extracted from HD-NNP, and the orange solid curves are from RPBE-DFT calculations. The green squares indicate the acoustic phonon modes obtained from experimental measurements (ref [41]). (b) Corresponding phonon density of states as a function of the frequency of phonon modes. (c) Variations of the reaction barrier height for the four representative dissociation geometries described in Figure 1a, with the vertical displacement of an individual Ru atom in the topmost surface layer. The plus markers indicate the reaction barrier heights calculated through DFT for the same barrier geometry as that found from HD-NNP. (d) Vertical shift of the barrier location along the molecular coordinate $Z$ as a function of the lattice coordinate $Q_\perp$.

obtained with high-resolution electron−electron-loss spectroscopy (30.4−32 meV).[46]

The good agreement between the NN and DFT descriptions of the phonons is not restricted to the depicted $\bar{\Gamma}-\bar{K}-\bar{M}-\bar{\Gamma}$ path; there is also excellent agreement between the RPBE-DFT and the HD-NNP results for the phonon density of states $g(\omega)$ for the calculations where all phonon modes in the surface Brillouin zone are taken into account (Figure 2b). The density function $g(\omega)$ also enables us to evaluate the effective Debye temperature $T_D$ of Ru(0001). To do this, the density of states for acoustic phonon modes needs to be fit as $g_D(\omega) \propto \omega^2$ within the Debye model. The resulting $T_D$ from the HD-NNP is 410 K, which agrees well with $T_D = 423$ K as obtained directly from our RPBE-DFT calculations and also with the values of 400−410 K obtained in low-energy electron diffraction measurements.[47,48] Altogether, the good agreement

noted between the HD-NNP and DFT suggests that the HD-NNP yields an accurate description of the lattice dynamics of the Ru(0001) surface.

To further validate the NN fit, we also examine the quality of the HD-NNP for the coupling between molecular and surface atom motion, at some stationary points. Starting from the ideal rigid Ru(0001) surface and using the HD-NNP, barrier geometries and heights are computed for the four $(X, Y, \varphi)$ dissociation geometries indicated in Figure 1a, through three-dimensional Newton−Raphson optimizations of $(r, Z, \theta)$ geometries. In Figure 2c, the coupling of the reaction barrier height $(E_b)$ to the motion of an individual Ru atom in the uppermost surface layer is investigated separately for the aforementioned dissociation geometries. Vertical displacements $(Q_\perp)$ of the surface Ru atom nearest to $N_2$ are considered. An approximation to $E_b$ is also calculated directly through DFT by computing the DFT energy for the molecular coordinates found from the HD-NNP and shown by "+" markers for reference. As seen, the barrier height exhibits roughly a linear dependence on $Q_\perp$, which agrees with the findings of similar studies on other adsorbate−surface systems.[49,50] In a similar vein, the vertical shift of the barrier location $Z_b$ along the molecular coordinate $Z$ also depends approximately linearly on $Q_\perp$, as illustrated in Figure 2d (in the procedure to obtain $Z_b$ through DFT calculations, the $r$ and $\theta$ coordinates were kept at the values obtained from the HD-NNP). In summary, and following the definitions of ref [49], the electronic coupling $\beta = -\Delta E_b/Q_\perp$ and the mechanical coupling $\alpha = \Delta Z_b/Q_\perp$, which can be taken as representative of the coupling between molecular and surface atom motion, are well described with the HD-NNP. This suggests that the HD-NNP may be used with confidence to assess the effects of surface temperature and of energy exchange with phonons on the dissociative chemisorption of $N_2$ on Ru(0001).

As a final test of the NN fit, we also checked whether the HD-NNP accurately describes the minimum barrier geometry and barrier height. For the HD-NNP, the minimum barrier geometry and height were found by performing a Newton−Raphson search incorporating all molecular coordinates but keeping the surface atoms fixed in their ideal geometry. The search was started from a bridge-to-hollow adsorption geometry as it was previously shown[20,40] that this dissociation geometry is close to the minimum barrier geometry. For comparison, we also calculated the minimum barrier coordinates and energy directly with RPBE-DFT using the climbing-image nudged elastic band[51] (CI NEB) technique. The results are summarized in Table 1. The barrier geometry and height derived from the HD-NNP are in excellent agreement with the raw DFT results.

We now turn to the effect of phonons on the reaction dynamics (Figure 3a,b). Comparisons were made with three types of experiments,[17,18] which we refer to here as Exps. 1−3. In Exp. 1, a nozzle temperature $(T_n)$ of 1100 K was used, and seeding with $H_2$ was carried out. The average collision energy was varied by changing the seeding ratio. Exp. 2 concerns a single experiment performed for $T_n = 1150$ K using He as a seeding gas. Both experiments were done by the same group and used $T_s = 575$ K for the surface (ref [18]). Careful error analysis was performed, estimating the extracted reaction probabilities to be accurate to within a factor 5. In Exp. 3 (ref [17]), $T_s = 600$ K and $T_n$ was varied between 350 and 1000 K to change the collision energy using seeding in $H_2$. The results were not accompanied by error analysis. We do not

**Table 1. Minimum Barrier Geometry and Its Height $E_b$ As Obtained from the HD-NNP and RPBE-DFT Calculations[a]**

| coordinates/height of barrier | HD-NNP | RPBE-DFT |
|---|---|---|
| $r$ (Å) | 1.738 | 1.741 |
| $Z$ (Å) | 1.312 | 1.318 |
| $X$ | 0.504 | 0.506 |
| $Y$ | 0.504 | 0.506 |
| $\theta$ | 84.3° | 84.0° |
| $\varphi$ | 30.0° | 30.0° |
| $E_b$ (eV) | 1.83 | 1.84 |

[a]For the RPBE-DFT calculations, the CI NEB method has been employed.
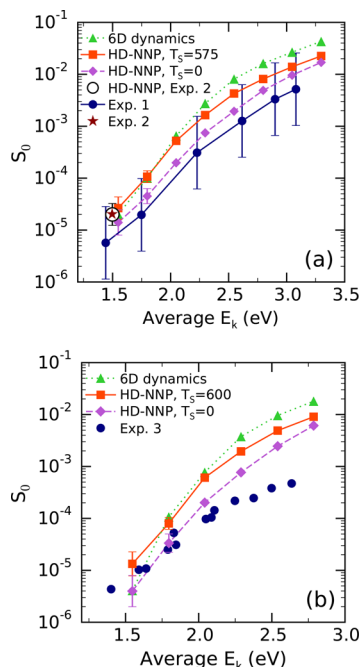


**Figure 3.** Dissociative sticking probability of $N_2$ on Ru(0001) as a function of its average translational energy. (a) Quasi-classical dynamics calculations are compared with two types of experiments[18] for $N_2$ beams seeded by $H_2$ (Exp. 1) and He (Exp. 2). The full squares indicate the sticking probability of $N_2$ for $T_s$ = 575 K including the effect of phonons (HD-NNP, $T_s$ = 575). The probability $S_0$ is also shown for $T_s$ = 0 with the surface treated as mobile (HD-NNP, $T_s$ = 0). The green triangles show the results obtained within the ideal rigid surface approximation (6D dynamics). (b) Same as that in (a), but the sticking probability is compared with experimental results of ref 17 (Exp. 3) for $T_s$ = 600 K.

consider the experiments performed by the same group and published in ref 16 as it is not clear how this group could have achieved collision energies as high as 4 eV with a hydrogen-seeded beam using $T_n$ up to 700 K (assuming an average translational energy of $2.7k_BT_n$ for $H_2$[52] and no velocity slip, the average collision energy could not have been higher than 2.3 eV in these experiments). When comparing our dynamics results to the experiments considered, we give the highest weight to Exps. 1 and 2 as they come with thorough error analysis.

In performing the dynamics calculations using the mobile surface, the seven-layer slab of Ru(0001) was first equilibrated to the surface temperature used in the experiments. The initial quantum states of $N_2$ were statistically populated in accordance with the value of $T_n$ used in the experiments, and our calculations mimic the velocity distribution of the molecular

beams in the experiments. In our quasi-classical dynamics calculations, dissociative chemisorption was operationally defined to occur once $r > 2.5r_{eq}$, where $r_{eq}$ = 1.117 Å denotes our RPBE value for the equilibrium N–N distance in the gas phase. In this study, $5 \times 10^5$ trajectories for incident energies of $E_k < 2$ eV and $10^5$ trajectories for $E_k \geq 2$ eV were run, ensuring statistically converged results over the incidence energy range of 1.5–3.25 eV. The outcome of our quasi-classical simulations is summarized in Figure 3. Taking into account the uncertainties in the reaction probabilities measured in Exp. 1, the calculated sticking probabilities $S_0$ computed with the RPBE functional are in good agreement with the experimental values (cf. the full squares and circles in Figure 3a), and the same holds true for Exp. 2 (cf. the blank circle and star marker). There are sizable discrepancies between the calculated results and the results of Exp. 3, especially for collision energies of >2.0 eV. However, as noted before, we attach greater weight to the comparison with the results of Exps. 1 and 2. Future calculations could assess the possible effects that electron–hole pair excitation might have on the calculated reaction probability. Most likely, their inclusion in the dynamical model should somewhat diminish the calculated reaction probabilities, although work in which the effect of their inclusion was investigated for similar systems suggests a much smaller role for electron–hole pair excitation than for the phonons for a similar $N_2$ + metal system.[3] Also, the error analysis of ref 18 clearly suggests that it would be worthwhile to invest efforts in improving the accuracy of the measurements for this paradigmatic reactive molecule–surface system.

The HD-NNP also allows us to assess the influence of surface temperature $T_s$ on the reactivity by comparing with $T_s$ = 0, that is, the Ru surface is static at the beginning of each trajectory but additionally accounts for energy dissipation into phonons during the collision of $N_2$ with the surface, as well as with 6D dynamics performed within the rigid surface approximation. As to the latter, we note that for the highest collision energy studied the rigid surface result overestimates the value obtained for $T_s$ = 575 K by more than a factor 2 (green triangles vs red squares). Clearly, allowing energy transfer from the molecule to the surface yields a decreased reaction probability. Compared to the 0 K simulations, raising $T_s$ to 575 K enhances the reaction probability by factors of 3–5 for incidence energies between 1.75 and 2.25 eV, emphasizing the need to model the effect of $T_s$ for this important reaction. We emphasize again that the HD-NNP allows us to study these effects and take them into account in comparing with experiment even for low collision energies where reaction probabilities are on the order $10^{-5}$–$10^{-4}$, which would at present have been impossible with AIMD simulations.

In summary, we have tested the applicability of a HD-NNP for describing the interaction of a molecule with a thermally distorted surface, taking the $N_2$ + Ru(0001) system, which is a paradigm of activated dissociative chemisorption, as an example. The HD-NNP fitted to RPBE-DFT calculations on this system accurately describes the lattice dynamics within the employed slab model of Ru(0001), the electronic and mechanical coupling between molecular and surface atom motion, and the interaction of the molecule with the metal surface. Furthermore, the HD-NNP allows sticking probabilities as small as $10^{-5}$ to be computed accurately in QCT calculations simulating both molecular and surface atom motion. Sticking probabilities computed with the HD-NNP are in good agreement with experimental molecular beam sticking proba-

bilities accompanied by a solid error analysis. The HD-NNP tested here allows accurate calculation of reaction probabilities for cases where these probabilities are too small for AIMD to be applicable.

## ■ ASSOCIATED CONTENT

### Ⓢ Supporting Information

The Supporting Information is available free of charge on the ACS Publications website at DOI: 10.1021/acs.jpclett.7b00784.

> Description of the electronic structure calculations, training data set for the neural network potential, construction of the HD-NNP, phonon calculations for Ru(0001), and quasi-classical simulations of $N_2$ dissociative adsorption on Ru(0001); convergence tests of the reaction barrier height (Table S1), parameters of radial and angular symmetry functions (Tables S2 and S3), 2D cut through the PES and sampling of $(r, Z)$ points (Figure S1), short-range radial and angular functions (Figure S2), velocity distribution characterizing the $N_2$ beam (Figure S3), and comparison of reaction probabilities for zero and small nonzero rotational temperatures (Figure S4) (PDF)

## ■ AUTHOR INFORMATION

### Corresponding Authors
*E-mail: k.shakouri@lic.leidenuniv.nl. Phone: +31 (0)71 527 4533. Fax: +31 (0)71 527 4397 (K.S.).
*E-mail: g.j.kroes@chem.leidenuniv.nl. Phone: +31 (0)71 527 4396. Fax: +31 (0)71 527 4397 (G.-J.K.).

### ORCID Ⓞ
Khosrow Shakouri: 0000-0002-5550-9731
Jörg Behler: 0000-0002-1220-1542
Jörg Meyer: 0000-0003-0146-730X
Geert-Jan Kroes: 0000-0002-4913-4689

### Notes
The authors declare no competing financial interest.

## ■ ACKNOWLEDGMENTS

## ■ REFERENCES

(1) Nave, S.; Jackson, B. Methane dissociation on Ni(111): The role of lattice reconstruction. *Phys. Rev. Lett.* **2007**, *98*, 173003.

(2) Nattino, F.; Costanzo, F.; Kroes, G. J. $N_2$ dissociation on W(110): An ab initio molecular dynamics study on the effect of phonons. *J. Chem. Phys.* **2015**, *142*, 104702.

(3) Novko, D.; Blanco-Rey, M.; Juaristi, J. I.; Alducin, M. Ab initio molecular dynamics with simultaneous electron and phonon excitations: Application to the relaxation of hot atoms and molecules on metal surfaces. *Phys. Rev. B: Condens. Matter Mater. Phys.* **2015**, *92*, 201411.

(4) Meyer, J.; Reuter, K. Modeling heat dissipation at the nanoscale: An embedding approach for chemical reaction dynamics on metal surfaces. *Angew. Chem., Int. Ed.* **2014**, *53*, 4721−4724.

(5) Busnengo, H. F.; di Césare, M. A.; Dong, W.; Salin, A. Surface temperature effects in dynamic trapping mediated adsorption of light molecules on metal surfaces: $H_2$ on Pd(111) and Pd(110). *Phys. Rev. B: Condens. Matter Mater. Phys.* **2005**, *72*, 125411.

(6) Groß, A.; Dianat, A. Hydrogen dissociation dynamics on precovered Pd surfaces: Langmuir is still right. *Phys. Rev. Lett.* **2007**, *98*, 206107.

(7) Nattino, F.; Galparsoro, O.; Costanzo, F.; Díez Muiño, R.; Alducin, M.; Kroes, G. J. Modeling surface motion effects in $N_2$ dissociation on W(110): Ab initio molecular dynamics calculations and generalized Langevin oscillator model. *J. Chem. Phys.* **2016**, *144*, 244708.

(8) Nattino, F.; Migliorini, D.; Kroes, G. J.; Dombrowski, E.; High, E. A.; Killelea, D. R.; Utz, A. L. Chemically accurate simulation of a polyatomic molecule-metal surface reaction. *J. Phys. Chem. Lett.* **2016**, *7*, 2402−2406.

(9) Kohn, W.; Sham, L. J. Self-consistent equations including exchange and correlation effects. *Phys. Rev.* **1965**, *140*, A1133−A1138.

(10) Kitano, M.; Kanbara, S.; Inoue, Y.; Kuganathan, N.; Sushko, P. V.; Yokoyama, T.; Hara, M.; Hosono, H. Electride support boosts nitrogen dissociation over ruthenium catalyst and shifts the bottleneck in ammonia synthesis. *Nat. Commun.* **2015**, *6*, 6731.

(11) Hellman, A.; Baerends, E. J.; Biczysko, M.; Bligaard, T.; Christensen, C. H.; Clary, D. C.; Dahl, S.; van Harrevelt, R.; Honkala, K.; Jonsson, H.; et al. Predicting catalysis: Understanding ammonia synthesis from first-principles calculations. *J. Phys. Chem. B* **2006**, *110*, 17719−17735.

(12) Diekhöner, L.; Mortensen, H.; Baurichter, A.; Luntz, A. C.; Hammer, B. Dynamics of high-barrier surface reactions: Laser-assisted associative desorption of $N_2$ from Ru(0001). *Phys. Rev. Lett.* **2000**, *84*, 4906−4909.

(13) Dahl, S.; Logadottir, A.; Egeberg, R. C.; Larsen, J. H.; Chorkendorff, I.; Törnqvist, E.; Nørskov, J. K. Role of steps in $N_2$ activation on Ru(0001). *Phys. Rev. Lett.* **1999**, *83*, 1814−1817.

(14) Murphy, M. J.; Skelly, J. F.; Hodgson, A.; Hammer, B. Inverted vibrational distributions from $N_2$ recombination at Ru(001): Evidence for a metastable molecular chemisorption well. *J. Chem. Phys.* **1999**, *110*, 6954−6962.

(15) Egeberg, R. C.; Larsen, J. H.; Chorkendorff, I. Molecular beam study of $N_2$ dissociation on Ru(0001). *Phys. Chem. Chem. Phys.* **2001**, *3*, 2007−2011.

(16) Romm, L.; Katz, G.; Kosloff, R.; Asscher, M. Dissociative chemisorption of $N_2$ on Ru(001) enhanced by vibrational and kinetic energy: Molecular beam experiments and quantum mechanical calculations. *J. Phys. Chem. B* **1997**, *101*, 2213−2217.

(17) Romm, L.; Citri, O.; Kosloff, R.; Asscher, M. A remarkable heavy atom isotope effect in the dissociative chemisorption of nitrogen on Ru(0001). *J. Chem. Phys.* **2000**, *112*, 8221−8224.

(18) Diekhöner, L.; Mortensen, H.; Baurichter, A.; Jensen, E.; Petrunin, V. V.; Luntz, A. C. $N_2$ dissociative adsorption on Ru(0001): The role of energy loss. *J. Chem. Phys.* **2001**, *115*, 9028−9035.

(19) Díaz, C.; Vincent, J. K.; Krishnamohan, G. P.; Olsen, R. A.; Kroes, G. J.; Honkala, K.; Nørskov, J. K. Multidimensional effects on dissociation of $N_2$ on Ru(0001). *Phys. Rev. Lett.* **2006**, *96*, 096102.

(20) Díaz, C.; Vincent, J. K.; Krishnamohan, G. P.; Olsen, R. A.; Kroes, G. J.; Honkala, K.; Nørskov, J. K. Reactive and nonreactive scattering of $N_2$ from Ru(0001): A six-dimensional adiabatic study. *J. Chem. Phys.* **2006**, *125*, 114706.

(21) Diekhöner, L.; Hornekær, L.; Mortensen, H.; Jensen, E.; Baurichter, A.; Petrunin, V. V.; Luntz, A. C. Indirect evidence for strong nonadiabatic coupling in $N_2$ associative desorption from and dissociative adsorption on Ru(0001). *J. Chem. Phys.* **2002**, *117*, 5018−5030.

(22) Behler, J.; Martonak, R.; Donadio, D.; Parrinello, M. Metadynamics simulations of the high-pressure phases of silicon employing a high-dimensional neural network potential. *Phys. Rev. Lett.* **2008**, *100*, 185501.

(23) Khaliullin, R. Z.; Eshet, H.; Kühne, T. D.; Behler, J.; Parrinello, M. Nucleation mechanism for the direct graphite-to-diamond phase transition. *Nat. Mater.* **2011**, *10*, 693−697.

(24) Gastegger, M.; Marquetand, P. High-dimensional neural network potentials for organic reactions and an improved training algorithm. *J. Chem. Theory Comput.* **2015**, *11*, 2187−2198.

(25) Wei, J. N.; Duvenaud, D.; Aspuru-Guzik, A. Neural networks for the prediction of organic chemistry reactions. *ACS Cent. Sci.* **2016**, *2*, 725−732.

(26) Natarajan, S. K.; Behler, J. Neural network molecular dynamics simulations of solid-liquid interfaces: Water at low-index copper surfaces. *Phys. Chem. Chem. Phys.* **2016**, *18*, 28704−28725.

(27) Jiang, B.; Li, J.; Guo, H. Potential energy surfaces from high fidelity fitting of ab initio points: The permutation invariant polynomial - neural network approach. *Int. Rev. Phys. Chem.* **2016**, *35*, 479−506.

(28) Lorenz, S.; Groß, A.; Scheffler, M. Representing high-dimensional potential-energy surfaces for reactions at surfaces by neural networks. *Chem. Phys. Lett.* **2004**, *395*, 210−215.

(29) Blank, T. B.; Brown, S. D.; Calhoun, A. W.; Doren, D. J. Neural network models of potential energy surfaces. *J. Chem. Phys.* **1995**, *103*, 4129−4137.

(30) Kolb, B.; Luo, X.; Zhou, X.; Jiang, B.; Guo, H. High-dimensional atomistic neural network potentials for molecule-surface interactions: HCl scattering from Au(111). *J. Phys. Chem. Lett.* **2017**, *8*, 666−672.

(31) Behler, J.; Parrinello, M. Generalized neural-network representation of high-dimensional potential-energy surfaces. *Phys. Rev. Lett.* **2007**, *98*, 146401.

(32) Behler, J. Atom-centered symmetry functions for constructing high-dimensional neural network potentials. *J. Chem. Phys.* **2011**, *134*, 074106.

(33) Behler, J. Representing potential energy surfaces by high-dimensional neural network potentials. *J. Phys.: Condens. Matter* **2014**, *26*, 183001.

(34) Hammer, B.; Hansen, L. B.; Nørskov, J. K. Improved adsorption energetics within density-functional theory using revised Perdew-Burke-Ernzerhof functionals. *Phys. Rev. B: Condens. Matter Mater. Phys.* **1999**, *59*, 7413−7421.

(35) Kresse, G.; Hafner, J. Ab initio molecular dynamics for liquid metals. *Phys. Rev. B: Condens. Matter Mater. Phys.* **1993**, *47*, 558−561.

(36) Kresse, G.; Hafner, J. Ab initio molecular-dynamics simulation of the liquid-metal amorphous-semiconductor transition in germanium. *Phys. Rev. B: Condens. Matter Mater. Phys.* **1994**, *49*, 14251−14269.

(37) Kresse, G.; Furthmüller, J. Efficiency of ab-initio total energy calculations for metals and semiconductors using a plane-wave basis set. *Comput. Mater. Sci.* **1996**, *6*, 15−50.

(38) Kresse, G.; Furthmüller, J. Efficient iterative schemes for ab initio total-energy calculations using a plane-wave basis set. *Phys. Rev. B: Condens. Matter Mater. Phys.* **1996**, *54*, 11169−11186.

(39) Behler, J. *RuNNer*, A program for constructing high-dimensional neural network potentials; Theoretische Chemie, Georg-August-Universität: Göttingen, Germany, 2017.

(40) Díaz, C.; Perrier, A.; Kroes, G. J. Associative desorption of $N_2$ from Ru(0001): A computational study. *Chem. Phys. Lett.* **2007**, *434*, 231−236.

(41) Braun, J.; Kostov, K. L.; Witte, G.; Surnev, L.; Skofronick, J. G.; Safron, S. A.; Wöll, C. Surface phonon dispersion curves for a hexagonally close packed metal surface: Ru(0001). *Surf. Sci.* **1997**, *372*, 132−144.

(42) Parlinski, K.; Li, Z. Q.; Kawazoe, Y. First-principles determination of the soft mode in cubic $ZrO_2$. *Phys. Rev. Lett.* **1997**, *78*, 4063−4066.

(43) Togo, A.; Tanaka, I. First principles phonon calculations in materials science. *Scr. Mater.* **2015**, *108*, 1−5.

(44) Meyer, J. *Ab initio modeling of energy dissipation during chemical reactions at transition metal surfaces*. Ph.D. thesis, Freie Universität Berlin, Germany, 2012.

(45) Plimpton, S. Fast parallel algorithms for short-range molecular dynamics. *J. Comput. Phys.* **1995**, *117*, 1−19.

(46) Heid, R.; Bohnen, K.-P.; Moritz, T.; Kostov, K. L.; Menzel, D.; Widdra, W. Anomalous surface lattice dynamics of a simple hexagonal close-packed surface. *Phys. Rev. B: Condens. Matter Mater. Phys.* **2002**, *66*, 161406.

(47) Schwegmann, S.; Seitsonen, A. P.; Dietrich, H.; Bludau, H.; Over, H.; Jacobi, K.; Ertl, G. The adsorption of atomic nitrogen on Ru(0001): Geometry and energetics. *Chem. Phys. Lett.* **1997**, *264*, 680−686.

(48) Michalk, G.; Moritz, W.; Pfnür, H.; Menzel, D. A LEED determination of the structures of Ru(001) and of CO/Ru(001)-$3^{1/2}\times 3^{1/2}$R30°. *Surf. Sci.* **1983**, *129*, 92−106.

(49) Nave, S.; Jackson, B. Methane dissociation on Ni(111) and Pt(111): Energetic and dynamical studies. *J. Chem. Phys.* **2009**, *130*, 054701.

(50) Bonfanti, M.; Díaz, C.; Somers, M. F.; Kroes, G. J. Hydrogen dissociation on Cu(111): The influence of lattice motion. Part I. *Phys. Chem. Chem. Phys.* **2011**, *13*, 4552−4561.

(51) Henkelman, G.; Uberuaga, B. P.; Jónsson, H. A climbing image nudged elastic band method for finding saddle points and minimum energy paths. *J. Chem. Phys.* **2000**, *113*, 9901−9904.

(52) Rettner, C. T.; Michelsen, H. A.; Auerbach, D. J. Quantum-state-specific dynamics of the dissociative adsorption and associative desorption of $H_2$ at a Cu(111) surface. *J. Chem. Phys.* **1995**, *102*, 4625−4641.